# ANALYSIS OF RATIONAL FUNCTION DEPENDENCY TO THE HEIGHT DISTRIBUTION OF GROUND CONTROL POINTS IN GEOMETRIC CORRECTION OF AERIAL AND SATELLITE IMAGES

M. Hosseini,

Department of Geomatics Engineering, Faculty of Engineering, Tehran University， hoseinm@ut.ac.ir
(Centre of Excellence for Geomatics Engineering & Natural Disasters Management)

**ABSTRACT:**

One of the existence mathematical models is Direct Linear Transformation (DLT). These equations are being regarded because of their simplicity as they are direct. When the height distribution of ground control points (GCPs) is inappropriate, height accuracy of DLT is low. This problem was not obvious about rational functions. To assess this case, the accuracy of rational functions has been tested in three different cases of GCPs distribution including over sampling, optimum sampling and under sampling. At last we have come to conclusions that the accuracy of rational functions in over sampling and optimum sampling are more than under sampling. But the accuracy of over sampling has not a significant difference with the accuracy of optimum sampling. In all cases, to compare the direct and indirect solution of rational function, we solved rational functions with both mentioned methods. At last it was clear that the accuracy of direct solution is more than the accuracy of indirect solution. All done tests are in terrain-dependent case of rational functions.

## 1 INTRODUCTION

There are a lot of mathematical models for photogrammetric processings. These models show the geometrical relationship between 2D image space and 3D ground space. Generally these models are divided to rigorous and generic models (McGlone, 1996). Selecting one of these models depends on the required accuracy and the available sensor ephemeris rigorous models are based on collinearity equations. One of the difficulties of rigorous models is their dependency to sensor. In other words these models have changed for different sensors. Because the number of different aerial and satellite sensors like frame, pushbroom and their applications are increasing, it is necessary that existed software be changed for the analysis of their different data. Also for using rigorous models it is necessary that imaging parameters like orbital parameters, satellite ephemeris, earth curvature, atmospheric refraction and lens distortion be known. It is essential that linearize these models because of their non-linearity. But generic models are in رایج تر because of its independence from position and orientation of sensor. Generally it isn't essential to know sensor's geometry for using generic models and it is possible to use them for different types of sensors. In generic models, relationship between image space and object space is making by rational functions.

## 2 RATIONAL FUNCTIONS

In rational functions, image pixel coordinates (r,c) are ratio of polynomials of ground coordinates (X,Y,Z) (OGC, 1999):

$$r_n = \frac{P1(X_n,Y_n,Z_n)}{P2(X_n,Y_n,Z_n)} = \frac{\sum_{i=0}^{m1}\sum_{j=0}^{m2}\sum_{k=0}^{m3} a_{ijk} X_n^i Y_n^j Z_n^k}{\sum_{i=0}^{n1}\sum_{j=0}^{n2}\sum_{k=0}^{n3} b_{ijk} X_n^i Y_n^j Z_n^k}$$

$$c_n = \frac{P3(X_n,Y_n,Z_n)}{P4(X_n,Y_n,Z_n)} = \frac{\sum_{i=0}^{m1}\sum_{j=0}^{m2}\sum_{k=0}^{m3} c_{ijk} X_n^i Y_n^j Z_n^k}{\sum_{i=0}^{n1}\sum_{j=0}^{n2}\sum_{k=0}^{n3} d_{ijk} X_n^i Y_n^j Z_n^k}$$

Where $r_n$ and $c_n$ are normalized row and column pixel coordinates in image space and Xn, Yn and Zn are normalized coordinates in ground space. For minimizing calculation errors, two iage coordinates and three ground coordinates are normalized such tha being in (-1,1) (NIMA, 2000).

$A_{ijk}$,, $b_{ijk}$, $c_{ijk}$ and $d_{ijk}$ are polynomial coordinates and were named rational function coefficients. For normalizing coordinates we can use below relations (OGC, 1999):

$$r_n = \frac{r - r_0}{r_s},\ c_n = \frac{c - c_0}{c_s},\ X_n = \frac{X - X_0}{X_s},$$

$$Y_n = \frac{Y - Y_0}{Y_s},\ Z_n = \frac{Z - Z_0}{Z_s}$$

Where $r_0$ and $c_0$ are image coordinate shifts and rs and cs are image coordinate scale numbers. Similarly, $X_0$, $Y_0$ and $Z_0$ are ground coordinate offsets and Xs, Ys and Zs are image coordinate scale numbers. Inverse rational functions are transformations from image space to ground space (Tao and Hu, 2001b):

$$X_n = \frac{P5(r_n,c_n,Z_n)}{P6(r_n,c_n,Z_n)}$$

$$Y_n = \frac{P7(r_n,c_n,Z_n)}{P8(r_n,c_n,Z_n)}$$

In these equations planimetric ground space coordinates (X,Y) are the ratio of polynomials of image pixel coordinates (r,c) and vertical ground coordinate (Z).

Rational function coefficients can be solved by sensor physical model or without it. If physical sensor model be known then we make a grid in image space. Then we used this grid and physical sensor models to produce another grid in 3D object space. Grid dimensions depend on ground dimensions and ground object's height differences. In other words grid dimensions fill all 3D ground space. This grid has many layers. Each layer points in each layer have the same elevation. Number of layers should be more than three to avoid rank deficiency of design matrix (Tao and Hu, 2000). After making the grid we had used ground coordinates with their similar image coordinates to calculate rational function coefficients by least square method. In this method there isn't any need to true ground information and it is named ground independent (Tao and Hu, 2000). This method were used for geometric correction of high resolution satellite images (Paderes et al., 1989; Madani, 1999; Yang et al., 2000; Baltsavias et al., 2001; Tao and Hu, 2000). We should know physical sensor model to produce 3D ground grid. For solving rational functions coefficients, we should used ground control points (GCPs) that were collected by general methods like map and DEM and calculating rational function coefficients. This method of solving rational functions was named terrain dependent (Tao and Hu, 2000). We used this method in remote sensing when physical sensor model is unknown (Toutin and Cheng, 2000; Tao and Hu, 2001a, b). There is limited research on solving rational functions by terrain dependent method that had done by Tao and Hu.

## 3 EXPERIMENT AND RESULTS

### 3.1 Simulated data set

For making simulated data set, first we suppose of a grid in ground space. Number of points should be sufficient. For calculating left and right image coordinates of ground points, we
used collinearity equations. Simulated is related to 1:10000 image scale. There totally 96 points that make a 12*8 grid. Figure 1 shows a 3D view of ground surface and these ground points. Heights of points had been choose such that the ground be approximately کوهستانی . Heights of points are between 10-100m.

Simulated data is related to 1:10000 image scale. There are totally 96 points that make a 12*8 grid. Figure 1 shows a 3D view of ground surface and these ground points. Heights of points have been chose such that the ground be nearly کوهستانی . They are between 10-100m. systematic error that have اعمال شدن is 10µm.

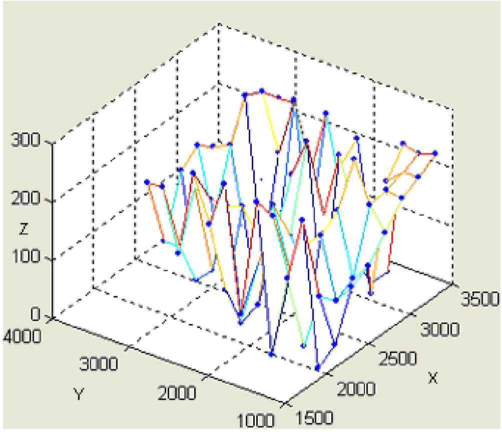


Figure1. Simulated ground points

### 3.2 Aerial data

In the next step, we used true aerial data for testing the models. These images are stereo that show a part of Germany. We used Softcopy for measuring ground control points' coordinates. These points are nearly a منظم grid and fill the entire image surface. Then we used collinearity equations with interior and exterior parameters to calculate image coordinates of ground points on stereo images. Calibrated focal length of the camera for taken aerial images is 152.844 and the approximate scale of these images is 1:15000. Figure 2 shows a 3D view of ground surface and extracted points. Maximum height difference of existed points is 120 meters.

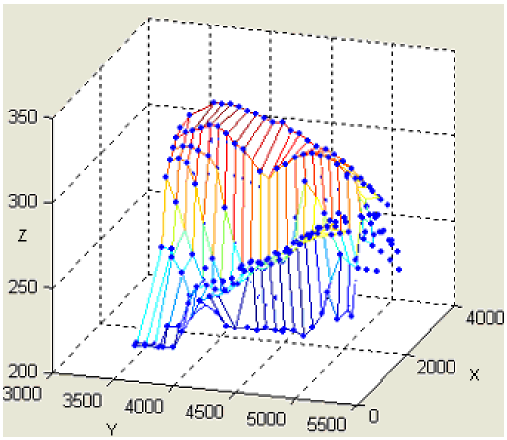


Figure2. Extracted ground points from aerial images

### 3.3 Space data

Stereo images had taken by IRS-1C satellite. These images show Mashhad city of Iran. Size of each image is 4096*4096 pixels and the overlap area of two images is 90 percents. There are 53 ground control points and their similar points in the images. Height of these points are between 930-1075m.

### 3.4 Results of simulated data

All the experiments have done in three different cases of control point's height distribution. We used terrain dependent rational functions in these experiments.

When we used optimum sampling we had GCPs in all places that there was high slope change. 3Ddistribution of control points were shown in figure 3. Number of control points are 56 and number of check points are 40. Model accuracies are shown in table 1. Regards to this table we can conclude:

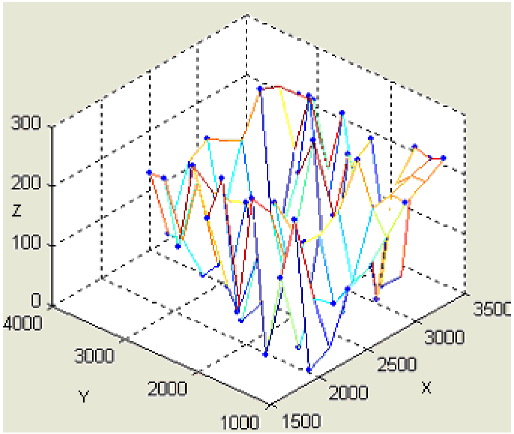


Figure 3. Ground control points distribution in optimum sampling

- When denominator of rational functions aren't equal ($P2 \neq P4$) the accuracies are more than when they are equal.
- Higher degree rational functions have more accuracy than low degrees.
- The accuracy of direct rational functions is more than the inverse one. But third order inverse rational functions have high accuracy too.

When are using oversampling there are GCPs in all places that there are high change slopes and in places between them. Number of control points are 88 and number of check points are 8. Distribution of control points were shown in figure 4.

Results of table 2 show that when we used oversampling the accuracies of the models are a little more from when we used optimum sampling but these differences aren't high.

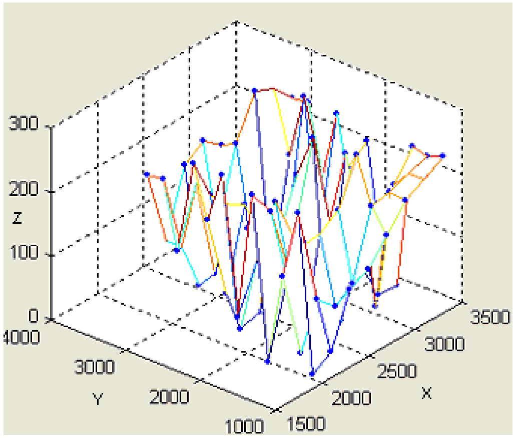


Figure 4. Ground control points distribution in over sampling

| | N.O.GCPs | N.O.CKPs | RMSECKPXYZ (cm) | RMSECNPXYZ (cm) |
|---|---|---|---|---|
| 1orderRFM(P2≠P4) | 56 | 40 | 5.946 | 6.178 |
| 2orderRFM(P2≠P4) | 56 | 40 | 1.261 | 0.617 |
| 3orderRFM(P2≠P4) | 56 | 40 | 1.349e-4 | 2.797e-5 |
| 2orderRFM(P2=P4) | 56 | 40 | 2.354 | 1.871 |
| 3orderRFM(P2=P4) | 56 | 40 | 0.503 | 0.308 |
| Inverse 1orderRFM (P2≠P4) | 56 | 40 | 487.040 | 471.593 |
| Inverse 2orderRFM (P2≠P4) | 56 | 40 | 1.548 | 1.343 |
| Inverse 3orderRFM (P2≠P4) | 56 | 40 | 0.0466 | 0.010 |

Table 1. Results obtained from simulated data in optimum sampling

| | N.O.GCPs | N.O.CKPs | RMSECKPXYZ (cm) | RMSECNPXYZ (cm) |
|---|---|---|---|---|
| 1orderRFM(P2≠P4) | 88 | 8 | 6.987 | 5.862 |
| 2orderRFM(P2≠P4) | 88 | 8 | 0.732 | 0.616 |
| 3orderRFM(P2≠P4) | 88 | 8 | 7.04e-5 | 3.57e-5 |
| 2orderRFM(P2=P4) | 88 | 8 | 2.040 | 1.891 |
| 3orderRFM(P2=P4) | 88 | 8 | 0.609 | 0.358 |
| Inverse 1orderRFM (P2≠P4) | 88 | 8 | 361.667 | 453.722 |
| Inverse 2orderRFM (P2≠P4) | 88 | 8 | 1.890 | 1.342 |
| Inverse 3orderRFM (P2≠P4) | 88 | 8 | 0.025 | 0.014 |

Table 2. Results obtained from simulated data in over sampling

When we use under sampling there isn't ground control points in all places of high slope and height distributions of control points are restricted. Number of ground control points are 44 and number of check points are 52. Figure 5 shows distribution of control points.

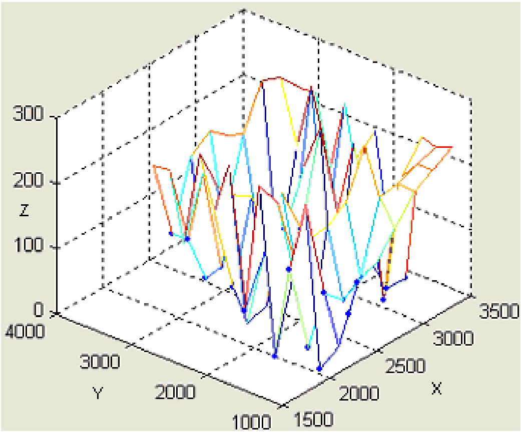


Figure 5. Ground control points distribution in under sampling

Results of the experiments were shown in table 3. Regards to this table we can conclude:

- Accuracies of check points have decreased in all models because control points hanven't good height distribution and all points are placed in low height levels. This shows that in under sampling case accuracies for check points aren't high.
- Approximately accuracies of control points have improved in all models because all control points are nearly in the same height level and fitting of rational functions to these points was better.
- By increasing rational functions' order, their accuracies have improved such that third order rational functions ( $P2 \neq P4$ ) have the best accuracy.

| | N.O.GCPs | N.O.CKPs | RMSECKPXYZ (cm) | RMSECNPXYZ (cm) |
|---|---|---|---|---|
| 1orderRFM(P2≠P4) | 44 | 52 | 8.410 | 5.235 |
| 2orderRFM(P2≠P4) | 44 | 52 | 50.041 | 0.960 |
| 3orderRFM(P2≠P4) | 44 | 52 | 1.407 | 0.006 |
| 2orderRFM(P2=P4) | 44 | 52 | 21.059 | 1.329 |
| 3orderRFM(P2=P4) | 44 | 52 | 6.707 | 0.021 |
| Inverse 1orderRFM (P2≠P4) | 44 | 52 | 1935.72 | 98.689 |
| Inverse 2orderRFM (P2≠P4) | 44 | 52 | 1014.16 | 2.496 |
| Inverse 3orderRFM (P2≠P4) | 44 | 52 | | |

Table 3. Results obtained from simulated data in under sampling

For the better analysis of residuals, first order rational functions error vectors of X, Y and Z elements in optimum sampling, over sampling and under sampling were shown in figure 6 and 7. For seeing error vectors more obvious, some of these vectors were shown. In all cases of sampling, rational functions' errors in Z direction are much more than X and Y directions, but the errors in X direction are the same as Y direction. Regarding these figures it can be see that maximum error is high, but we saw in previous tables, the average error of first order ational functions is approximately 6cm for optimum sampling and over sampling and the error is nearly 10cm for under sampling.

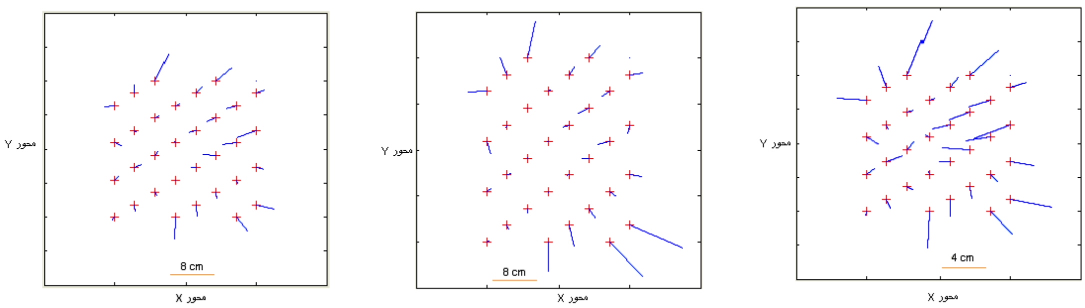


(a) (b) (c)

Figure 6. Planimetric error vectors of first order rational functions in a) optimum sampling b) over sampling c) under sampling

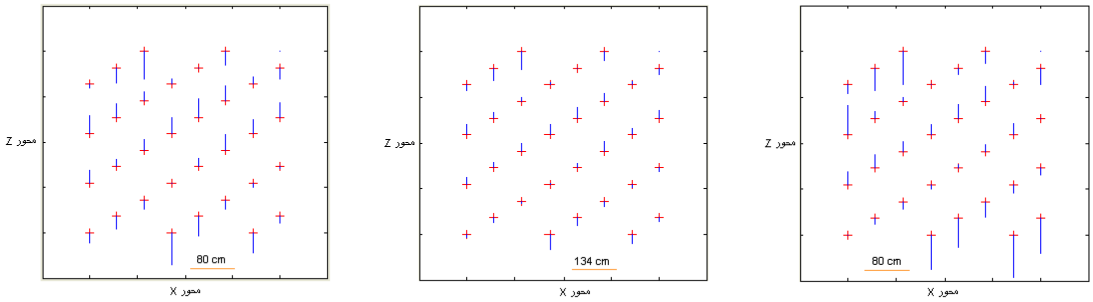


(a) (b) (c)

Figure 7. Height error vectors of first order rational functions in a) optimum sampling b) over sampling c) under sampling

### 3.5 Results of aerial images

In optimum sampling, we have chose 71 GCPs and 234 check points. Distribution of control points were shown in figure 8.

Regarding table 4 we can conclude:

- Accuracy of rational functions in $P2 \neq P4$ is more than $P2 = P4$
- Accuracy of direct rational functions are more than inverse rational functions for first and second orders but the differences are not high for third order rational functions.

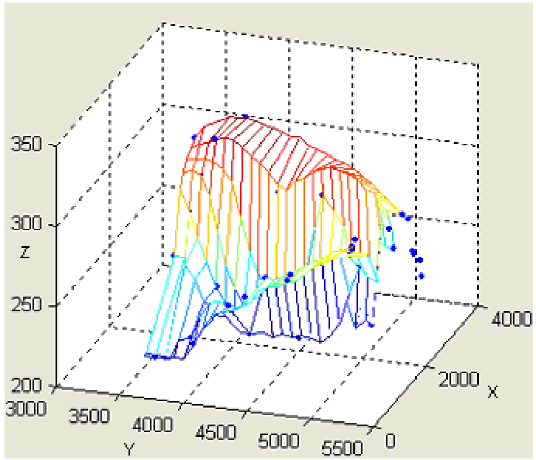


Figure 8. Ground control points distribution in optimum sampling

| | N.O.GCPs | N.O.CKPs | RMSECKPXYZ (cm) | RMSECNPXYZ (cm) |
|---|---|---|---|---|
| 1orderRFM(P2≠P4) | 71 | 234 | 5.572 | 6.026 |
| 2orderRFM(P2≠P4) | 71 | 234 | 0.803 | 0.726 |
| 3orderRFM(P2≠P4) | 71 | 234 | 0.036 | 0.013 |
| 2orderRFM(P2=P4) | 71 | 234 | 3.220 | 2.290 |
| 3orderRFM(P2=P4) | 71 | 234 | 0.142 | 0.055 |
| Inverse 1orderRFM (P2≠P4) | 71 | 234 | 64.848 | 64.530 |
| Inverse 2orderRFM (P2≠P4) | 71 | 234 | 3.878 | 2.925 |
| Inverse 3orderRFM (P2≠P4) | 71 | 234 | 0.022 | 0.008 |

Table 4. Results obtained from aerial data in optimum sampling

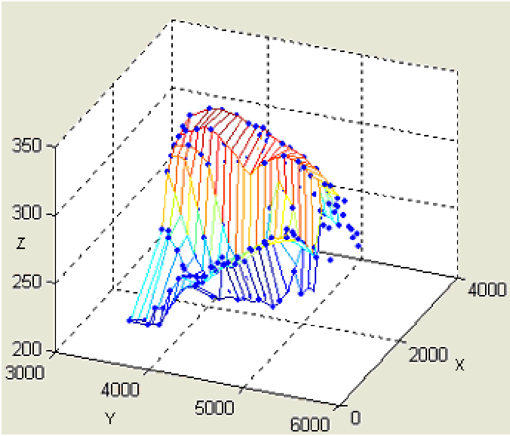


Figure 9. Ground control points distribution in over sampling

Number of points that we have chose in over sampling are 185 GCPs and 120 check points. 3D distribution of ground control points were shown in figure 9.

Regards to table 5, accuracies of all models are more than optimum sampling. Other results are the same as optimum sampling

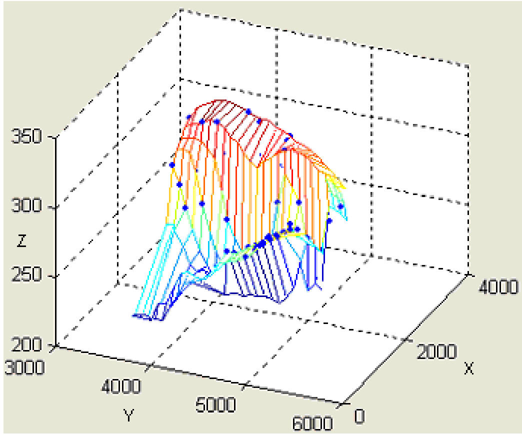


Figure 10. Ground control points distribution in under sampling

Number of points in under sampling are 60 GCPs and 245 check points. Distribution of GCPs were shown in figure 10.

Results of experiments were reported in table 6. Regards to this table, accuracies of models are much degraded on check points respect to over sampling and under sampling but accuracies are increased on GCPs. Other results are the same as other sampling cases.

| | N.O.GCPs | N.O.CKPs | RMSECKPXYZ (cm) | RMSECNPXYZ (cm) |
|---|---|---|---|---|
| 1orderRFM(P2≠P4) | 185 | 120 | 4.680 | 5.505 |
| 2orderRFM(P2≠P4) | 185 | 120 | 0.676 | 0.976 |
| 3orderRFM(P2≠P4) | 185 | 120 | 0.020 | 0.022 |
| 2orderRFM(P2=P4) | 185 | 120 | 2.150 | 2.308 |
| 3orderRFM(P2=P4) | 185 | 120 | 0.080 | 0.086 |
| Inverse 1orderRFM (P2≠P4) | 185 | 120 | 60.705 | 64.281 |
| Inverse 2orderRFM (P2≠P4) | 185 | 120 | 2.202 | 2.473 |
| Inverse 3orderRFM (P2≠P4) | 185 | 120 | 0.010 | 0.010 |

Table 5. Results obtained from aerial data in over sampling

| | N.O.GCPs | N.O.CKPs | RMSECKPXYZ (cm) | RMSECNPXYZ (cm) |
|---|---|---|---|---|
| 1orderRFM(P2≠P4) | 60 | 245 | 14.919 | 2.890 |
| 2orderRFM(P2≠P4) | 60 | 245 | 9.342 | 0.520 |
| 3orderRFM(P2≠P4) | 60 | 245 | 0.613 | 0.005 |
| 2orderRFM(P2=P4) | 60 | 245 | 18.367 | 0.990 |
| 3orderRFM(P2=P4) | 60 | 245 | 1.129 | 0.036 |
| Inverse 1orderRFM (P2≠P4) | 60 | 245 | 143.310 | 17.596 |
| Inverse 2orderRFM (P2≠P4) | 60 | 245 | 29.040 | 0.980 |
| Inverse 3orderRFM (P2≠P4) | 60 | 245 | 0.431 | 0.004 |

Table 6. Results obtained from aerial data in under sampling

First order rational functions error vectors of X, Y and Z elements in optimum sampling, over sampling and under sampling were shown in figure 11 and 12. Some of these vectors were eliminated to the figures be more obvious. For aerial data like simulated data, rational functions' errors in Z direction are much more than X and Y directions for all three sampling cases but the amounts of errors in X and Y directions are the same. As can be seen, maximum error is high but by regards prvious tables, check points average errors of first order rational functions are nearly 5.5cm for optimum sampling, 5cm for over sampling and 15cm for under sampling.

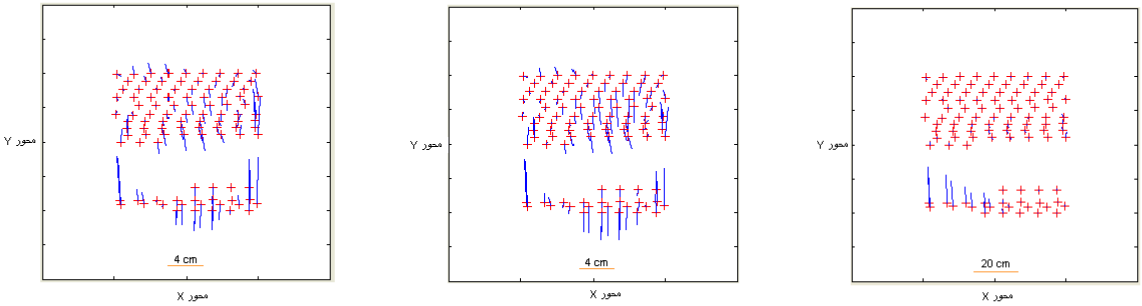


(a) (b) (c)

Figure 11. Planimetric error vectors of first order rational functions in a) optimum sampling b) over sampling c) under sampling

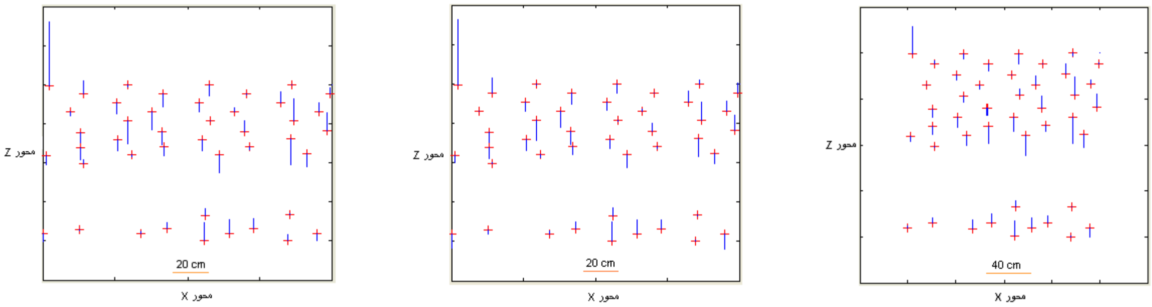


(a) (b) (c)

Figure 12. Height error vectors of first order rational functions in a) optimum sampling b) over sampling c) under sampling

### 3.6 Results of space data

Because of there wasn't enough control points, we have done the experiments for only under sampling. The results were shown in table 7. Number of points are 30 GCPs and 14 check points. Regards to table 7 we can conclude:

- Accuracy of first and second order rational functions are more than third orders.
- Accuracies in $P2 \neq P4$ is much more than $P2 = P$
- Direct rational functions are دقیقتر than inverse ones

| | N.O.GCPs | N.O.CKPs | RMSECKPXYZ (m) | RMSECNPXYZ (m) |
|---|---|---|---|---|
| 1orderRFM(P2≠P4) | 39 | 14 | 14.349 | 10.642 |
| 2orderRFM(P2≠P4) | 39 | 14 | 26.717 | 12.933 |
| 3orderRFM(P2≠P4) | 39 | 14 | 59.088 | 35.115 |
| 2orderRFM(P2=P4) | 39 | 14 | 68.162 | 24.941 |
| 3orderRFM(P2=P4) | 39 | 14 | 136.356 | 61.126 |
| Inverse 1orderRFM (P2≠P4) | 39 | 14 | 16.698 | 12.543 |
| Inverse 2orderRFM (P2≠P4) | 39 | 14 | 34.412 | 235.479 |
| Inverse 3orderRFM (P2≠P4) | 39 | 14 | 125.155 | 249.016 |

Table 6. Results obtained from space data in under sampling

Planimetric and height error vectors were shown in figures 13 and 14. For seeing error vectors more obvious, some of these vector were eliminated.

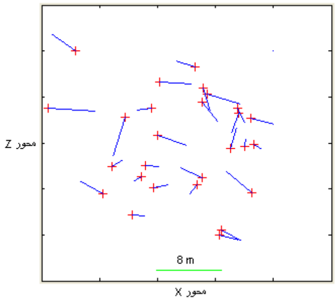


Figure 13. Planimetric error vectors of first order rational functions

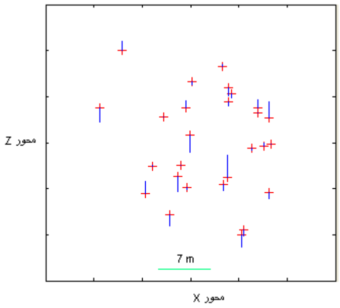


Figure 14. Height error vectors of first order rational functions

## 4 CONCLUSION

For the analysis of dependence of rational functions and height distribution of control points, their accuracies were analyzed in three different cases of control points height distribution. At last we saw that rational functions are dependent to height distribution of control points and accuracies in under sampling are much degraded but because of the accuracies in over sampling and optimum sampling aren't too different, using over sampling for rational functions are not necessary

## REFERENCES


1- McGlone, C., 1996 :"Sensor modeling in image registration," Digital Pgotogrammetry : An Addendum (C. W. Greve, editor), American Society for Photogrammetry and Remote Sensing, Bethesda, Maryland, pp. 115-123.

2- Paderes, Jr., F. C., Mikhail, E. M., Fagerman, J. A., 1989. Batch and on-line evalution of stereo SPOT imagery, Proceedings of the ASPRS-ACSM Convention, Baltimore, April, pp. 31-40.

3- Yang, X., 2000 : "Accuracy of rational function approximation in photogrammetry," Proceedings of ASPRS Annual Convention, Washington D.C. May 22-26.

4- Baltsavias, E., Pateraki, M., and Zhang, L., 2001, Radiometric and geometric evaluation of IKONOS Geo images and their use for 3D building modeling. Proceedings of Joint ISPRS Workshop High Resolution Mapping from Space 2001, 19-21 September (Hannover: International Society of Photogrammetry and Remote sensing (CD-ROM)), pp. 15-35.

5- Toutin, T., Cheng, P., 2000. Demystification of IKONOS Earth Observation Magazine (EOM), 9(7): 17-21.

6- OpenGIS Consortium, 1999. The OpenGIS Abstract Specification – Topic 7: The Earth Imagery Case, http://www.opengis.org/public/abstract/99-107.pdf.

7- NIMA., 2000 : "The compendium of controlled extensions (CE) for the national imagery transmission format (NITF), version 2.1.

8- Tao, C. V., Hu, Y., 2000: "A Comprehensive Study on the Rational Function Model for Photogrammetric Processing," Photogrammetric Engineering and Remote Sensing.

9- Tao, C. V., Hu, Y., 2001a : "The rational function model – a tool for processing high-resolution imagery," Earth Observation Magazine (EOM), 10(1) : 13-16.

10- Tao, C. V., Hu, Y., 2001b : "3-D Reconstruction Algorithms based on the Rational Function Model," Proceeding of Joint ISPRS Workshop on "High Resolution Mapping from Space 2001," Hannover, September 19-21.

11- Madani, M., 1999 : "Real-time sensor-independent positioning by rational functions," Proceedings of ISPRS Workshop on "Direct versus indirect Methods of Sensor Orientation," 25-26 November, Barcelona, Spain, pp. 64-75.